This is a previous version of the article published in Journal of Dynamic Systems, Measurement, and Control. 2024, 146(2): 024501. https://doi.org/10.1115/1.4063907

Flatness-based control in successive loops for autonomous quadrotors

G. Rigatos[a] M. Abbaszadeh[b] K. Busawon[c]

[a]Unit Industrial Autom.
Industrial Systems Inst.
26504, Patras, Greece
grigat@ieee.org

[b]Dept. ECS Engineering
Rensselaer Polytech. Inst.
12065, NY, USA
masouda@ualberta.ca

[c]Nonlinear Control Group
Univ. of Northumbria
Newcastle NE1 8ST, UK
krishna.busawon@northumbria.ac.uk

L. Dala[d] J. Pomares[e] F. Zouari[f]

[d] Dept. of Mechanical Eng.
Univ. of Northumbria
Newcastle NE1 8ST, UK
laurent.dala@nirthumbrua.ac.uk

[e]Dept. of Systems Eng
Univ. of Alicante
03690, Alicante, Spain
jpomares@gcloud.ua.es

[f]Lab. d' Automatique
Ecole d' Ingénieurs de Tunis
Belvédêre, 1002 Tunis, Tunisie
zouari.farouk@gmail.com

Abstract: The control problem for the multivariable and nonlinear dynamics of unmanned rotorcrafts is treated with the use of a flatness-based control approach which is implemented in successive loops. The state-space model of 6-DOF autonomous quadrotors is separated into two subsystems, which are connected between them in cascading loops. Each one of these subsystems can be viewed independently as a differentially flat system and control about it can be performed with inversion of its dynamics as in the case of input-output linearized flat systems. The state variables of the second subsystem become virtual control inputs for the first subsystem. In turn, exogenous control inputs are applied to the second subsystem. The whole control method is implemented in two successive loops and its global stability properties are also proven through Lyapunov stability analysis. The validity of the control method is further confirmed through simulation experiments showing precise tracking of 3D flight paths by the 6-DOF quadrotor.

Keywords: unmanned aerial vehicles, quadrotors, multivariable control, differential flatness properties, flatness-based control in successive loops, global stability, Lyapunov analysis.

1 Introduction

Research on control of nonlinear dynamical systems has grown significantly during the last years, with differential flatness theory to have a major contribution in the development of related results and solutions for nontrivial control problems [1-8]. Differential flatness properties are confirmed for a dynamical system if all its state variables and its control inputs can be expressed as functions of algebraic variables which constitute the so-called flat outputs vector, and also as functions of the flat-output vector's derivatives [9-12]. The differential flatness property enables the transformation of the nonlinear system's dynamics in the linear canonical form [13-17]. The latter description is controllable and observable thus allowing to treat effectively control and estimation problems [18-21]. In this paper, a successive loops approach is developed for controller design in nonlinear dynamical systems which exhibit the differential flatness property. The method makes use of the initial nonlinear model of the system and of its decomposition into

a set of nonlinear subsystems for which the differential flatness property holds [29-30].

Usually, through successive differentiations of its flat outputs a differentially flat dynamical system can be transformed through successive differentiations of its flat outputs into the input-output linearized form and subsequently into the canonical Brunovsky form [22- 24] . Because quadrotors are underactuated systems, this linearization process through successive differentiations will also need to extend the state-space model of these systems by applying the dynamic extension principle and by considering as additional state variables some of the systems' inputs and their time derivatives [24-28]. The canonical state-space description is both controllable and observable. Therefore one can argue that the control and state-estimation problems for differentially flat systems can be easily solved once their transformation into the canonical state-space description is completed. However, one has to perform also inverse transformations so as to return to the initial nonlinear state-space model of the system. These transformations may come against singularity (non-invertibility) issues. On the other side, in the article's flatness-based control method in successive loops there are no changes of state variables, no transformations of the state-space model of the controlled system and back and forth transformations, and consequently the occurrence of singularities should be excluded.

The present article treats the control and trajectories tracking problem for 6-DOF unmanned quadropters with the use of a flatness-based control approach which is implemented in successive loops. This control problem is nontrivial due to the strong nonlinear dynamics and the multivariable form that characterizes the associated state-space description. The state-space model of the 6-DOF autonomous quadropters is separated into two subsystems, which are connected between them in cascading loops. By proving that differential flatness properties hold for each one of these subsystems it is confirmed that a stabilizing feedback controller can be designed for each one of them through inversion of their dynamics. The state vector of the subsequent (i+1-th) subsystem becomes virtual control input to the preceding (i-th) subsystem. Equivalently, the virtual control input of the preceding (i-th) subsystem becomes setpoint for the subsequent (i+1-th) subsystem. From the last subsystem one computes the real control inputs which should be applied to this aerial drone by tracing backwards the virtual control inputs for all previous subsystems. The global stability properties of the control scheme are proven through Lyapunov analysis. The method is easy to implement since to stabilize the unmanned aerial vehicle it suffices to define for each one of its subsystems a positive diagonal gain matrix.

The new solution of the motion control and trajectory tracking problem of 6-DOF unmanned quadrotors is a meaningful result. Such a type of drones finds also ample use in several civilian, security and military applications. The motion of the 6-DOF quadropter can be described using either an inertial reference frame or a body-fixed frame [31-32]. In the inertial reference frame the quadrotor's motion is defined by a vector of three cartesian coordinates and by a vector of three Euler angles (rotation angles) of the drone around the axes of the inertial reference system [33-34]. In the body-fixed frame the quadrotor's motion is defined by a vector of three linear velocities and by a vector of three angular velocities which express rotation around the axes of the body-fixed reference system [35-36]. Transition from the description in the inertial reference frame to the description in the body-fixed frame and inversely is performed with suitable rotation matrices [37-38]. The dynamic model of the 6-DOF quadrotor is underactuated, which imposes an additional level of difficulty in the solution of the associated control problem [39-41]. There are six-degrees of freedom (out of which three describe translational motion and three describe rotational motion) while the drone's dynamic model receives only four control inputs (a lift force and three torques which define the turn angles of the quadropter) [42-43]. The complete 6-DOF dynamic model of the quadrotor is a highly nonlinear one and its control is usually performed with (i) global linearization control methods [44- 45], (ii) local linearization control methods [46-48] and (iii) Lyapunov analysis-based methods [49-51]. The present article demonstrates solution of the nonlinear control problem of 6-DOF unmanned quadrotors with the use of flatness-based control implemented in successive loops.

The structure of the article is as follows: In Section 2, the dynamic model of 6-DOF autonomous quadrotors is analyzed. In Section 3, flatness-based control in successive loops is developed for the dynamic model of 6-DOF unmanned quadrotors. In Section 4, simulation tests are performed to further confirm the global stability properties and the fine tracking performance of flatness-based control in successive loops for 6-DOF unmanned quadrotors. Moreover, in Section 5, concluding remarks are stated.

2 Dynamic model of 6-DOF quadrotors

The considered problem is that of control of the quadrotor in a 6 degrees of freedom motion. The first three degrees of freedom describe translational motion of the quadrotor in the xyz cartesian space, along the x-axis, the y-axis and the z-axis. The rest three degrees of freedom describe rotational motion of the quadrotor around the axes of the inertial reference frame. Considering as state variables (a) the x, y and z-axis position of the UAV, (b) the rotation angles of the drone ϕ, θ and ψ around the axes of the inertial reference frame, (c) the linear angular velocities of the UAV $\dot{x}$, $\dot{y}$ and $\dot{z}$ along the axes of inertial frame and finally (d) the angular velocities of the UAV $\dot{\phi}$, $\dot{\theta}$, and $\dot{\psi}$ around the axes of the inertial coordinates system, the resulting state-space model is of dimension 12, while receiving only four control inputs. The four control inputs of the quadrotor are a thrust force that can lift up the drone and torques generated by the unequal turn speeds of its rotors that can change the position of the quadrotor's center of gravity or can change its orientation angles with respect to the axes of the inertial reference frame. The quadrotor's model is nonlinear and underactuated and the solution of the associated control problem is a nontrivial task.

The kinematic and dynamic model of the quadrotor can be described with the use of a body-fixed frame and an inertial reference frame. The body-fixed frame is denoted as $OXYZ$ and describes the position of the quadrotor in the cartesian space $\xi = [x, y, z]^T$, as well as the quadrotor's attitude which is described by the Euler angles vector $\eta = [\phi, \theta, \psi]^T$ (rotation angles around axes OX, OY and OZ respectively). The body-fixed frame is denoted as $OB_1B_2B_3$ and describes linear velocities $V_B = [u, v, w]^T$, as well as rotation velocities $\omega = [p, q, r]^T$ in this coordinates system [1], [2].

The linear velocities vector of the quadrotor in the inertial frame is denoted by $V_E = [\dot{x}, \dot{y}, \dot{z}]^T$ and is related with the velocities vector in the body-fixed frame $V_B = [u, v, w]^T$ through the following equation [1], [2]

$$V_E = RV_B \tag{1}$$

where rotation matrix R is given by

$$R = \begin{pmatrix} C\psi C\theta & C\psi S\theta S\phi - S\psi C\phi & C\psi S\theta C\phi + S\psi S\phi \\ S\psi C\theta & S\psi S\theta S\phi + C\psi C\phi & S\psi S\theta C\phi - C\psi S\phi \\ -S\theta & C\theta S\phi & C\theta C\phi \end{pmatrix} \tag{2}$$

where $C = cos(\cdot)$ and $S = sin(\cdot)$. The angular velocities of the quadrotor in the inertial frame $\dot{\eta} = [\dot{\phi}, \dot{\theta}, \dot{\psi}]^T$ and the angular velocities in the body-fixed frame $\omega = [p, q, r]^T$ are connected through the relation

$$\dot{\eta} = W^{-1}\omega \tag{3}$$

that is [1], [2]

$$\begin{pmatrix} \dot{\phi} \\ \dot{\theta} \\ \dot{\psi} \end{pmatrix} = \begin{pmatrix} 1 & sin(\phi)tan(\theta) & cos(\phi)tan(\theta) \\ 0 & cos(\phi) & -sin(\phi) \\ 0 & sin(\phi)sec(\theta) & cos(\phi)sec(\theta) \end{pmatrix} \begin{pmatrix} p \\ q \\ r \end{pmatrix} \tag{4}$$

The Euler-Lagrange equation for the quadropter is formulated as follows

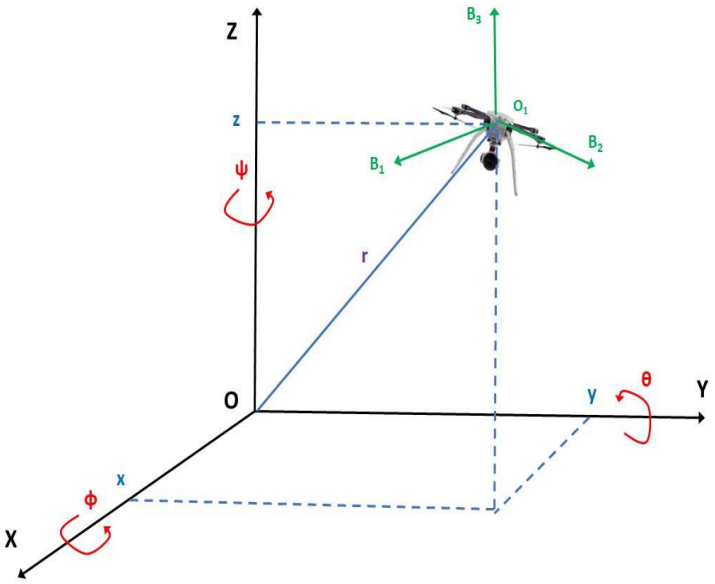

Figure 1: Inertial and body-fixed reference frames for the 6-DOF quadropter

$$\frac{d}{dt}\left(\frac{\partial L}{\partial \dot{q}_i}\right) - \frac{\partial L}{\partial q_i} = \begin{pmatrix} f_\xi \\ \tau_\eta \end{pmatrix} \tag{5}$$

where the Lagrangian is defined as $L(q,\dot{q}) = E_{C_{tr}} + E_{C_{rot}} - E_p$, $E_{C_{tr}}$ is the kinetic energy of the quadrotor due to translational motion, $E_{C_{rot}}$ is the kinetic energy of the quadrotor due to rotational motion and E_p is the total potential energy of the quadrotor due to lift. The generalized state vector is $q = [\xi^T, \eta^T]^T \in R^6$, $\tau_\eta \in R^3$ is the torques vector that causes rotation round the axes of the body-fixed reference frame, and $f_\xi = R\hat{f} + \alpha_T$ is the translational forces vector applied to the quadropter due to the main control input U_1, while $\alpha_T = [A_x, A_y, A_z]^T$ is the aerodynamic forces vector, defined along the axes of the inertial reference frame. Since the Lagrangian does not contain cross-coupling between the $\dot{\xi}$ and the $\dot{\eta}$ terms, the Lagrange-Euler equations can be divided into translational and rotational dynamics.

Euler-Lagrange analysis for the qusdrotor	
Parameter	*Definition*
$L(q,\dot{q}) = E_{C_{tr}} + E_{C_{rot}} - E_p$	Lagrangian of the quadrotor
$E_{C_{tr}}$	kinetic energy due to translational motion
$E_{C_{rot}}$	kinetic energy due to rotational motion
E_p	total potential energy due to lift
$q = [\xi^T, \eta^T]^T \in R^6$	generalized state vector
$\xi \in R^3$	Cartesian coordinates vector
$\eta \in R^3$	rotation angles vector in inertial frame
$\tau_\eta \in R^3$	torques' vector
$f_\xi = R\hat{f} + \alpha_T$	translational forces vector
$\alpha_T = [A_x, A_y, A_z]^T$	aerodynamic forces vector

The translational dynamics of the quadropter is given by

$$m\ddot{\xi} + mge_3 = f_\xi \tag{6}$$

where $e_3 = [0, 0, 1]^T$ is the unit vector along the z axis of the inertial reference frame. Eq. (6) can be written using the following three equations [1], [2]:

$$\begin{array}{c} \ddot{x} = \frac{1}{m}(cos(\psi)sin(\theta)cos(\phi) + sin(\psi)sin(\phi))U_1 + \frac{A_x}{m} \\ \ddot{y} = \frac{1}{m}(sin(\psi)sin(\theta)cos(\phi) - cos(\psi)sin(\phi))U_1 + \frac{A_y}{m} \\ \ddot{z} = -g + \frac{1}{m}(cos(\theta)cos(\phi))U_1 + \frac{A_z}{m} \end{array} \tag{7}$$

where m is the quadropter's mass and g is the gravitational acceleration. The rotational dynamics of the quadropter is given by [1], [2]

$$M(\eta)\ddot{\eta} + C(\eta, \dot{\eta})\dot{\eta} = \tau_\eta \tag{8}$$

where the inertia matrix $M(\eta)$ is defined as

$$M(\eta) = \begin{pmatrix} I_{xx} & 0 & -I_{xx}S\theta \\ 0 & I_{yy}C^2\phi + I_{zz}S^2\phi & (I_{yy} - I_{zz})C\phi S\phi C\theta \\ -I_{xx}S\theta & (I_{yy} - I_{zz})C\phi S\phi C\theta & I_{xx}S^2\theta + I_{yy}S^2\phi C^2\theta + I_{zz}C^2\phi C^2\theta \end{pmatrix} \tag{9}$$

and the Coriolis matrix is

$$C(\eta, \dot{\eta}) = \begin{pmatrix} c_{11} & c_{12} & c_{13} \\ c_{21} & c_{22} & c_{23} \\ c_{31} & c_{32} & c_{33} \end{pmatrix} \tag{10}$$

where the elements of the matrix are

$$\begin{array}{l} c_{11} = 0 \\ c_{12} = (I_{yy} - I_{zz})(\dot{\theta}C\phi S\phi + \dot{\psi}S^2\phi C\theta) + (I_{zz} - I_{yy})\dot{\psi}C^2\phi C\theta \\ c_{13} = (I_{zz} - I_{yy})\dot{\psi}C\phi S\phi C^2\theta \\ c_{21} = (I_{zz} - I_{yy})(\dot{\theta}C\phi S\phi + \dot{\psi}S^2\phi C\theta) + (I_{yy} - I_{zz})\dot{\psi}C^2\phi C\theta + I_{xx}\dot{\psi}C\theta \\ \\ c_{22} = (I_{zz} - I_{yy})\dot{\phi}C\phi S\phi \\ c_{23} = -I_{xx}\dot{\psi}S\theta C\theta + I_{yy}\dot{\psi}S^2\phi C\theta S\theta + I_{zz}\dot{\psi}C^2\phi S\theta C\theta \\ c_{31} = (I_{yy} - I_{zz})\dot{\psi}C^2\theta S\phi C\phi - I_{xx}\dot{\theta}C\theta \\ c_{32} = (I_{zz} - I_{yy})(\dot{\theta}C\phi S\phi S\theta + \dot{\phi}S^2\phi C\theta) + (I_{yy} - I_{zz})\dot{\phi}C^2\phi C\theta + I_{xx}\dot{\psi}S\theta C\theta - \\ -I_{yy}\dot{\psi}S^2\phi S\theta C\theta - I_{zz}\dot{\psi}C^2\phi S\theta C\theta \\ c_{33} = (I_{yy} - I_{zz})\dot{\phi}C\phi S\phi C^2\theta - I_{yy}\dot{\theta}S^2\phi C\theta S\theta - \\ -I_{zz}\dot{\theta}C^2\phi C\theta S\theta + I_{xx}\dot{\theta}C\theta S\theta \end{array} \tag{11}$$

Thus, the mathematical model that describes the quadrotor's rotational motion is given by [1], [2]

$$\ddot{\eta} = -C(\eta, \dot{\eta})\dot{\eta} + M(\eta)^{-1}\tau_\eta \tag{12}$$

In the relations describing the translational motion of the quadrotor, given in Eq. (7) one defines the following control inputs:

$$\begin{array}{c} v_1 = \frac{1}{m}(cos(\psi)sin(\theta)cos(\phi) + sin(\psi)sin(\phi))U_1 \\ v_2 = \frac{1}{m}(sin(\psi)sin(\theta)cos(\phi) - cos(\psi)sin(\phi))U_1 \\ v_3 = -g + \frac{1}{m}(cos(\theta)cos(\phi))U_1 \end{array} \tag{13}$$

After intermediate algebraic operations one can confirm that the following relations hold

$$v_1^2 + v_2^2 + (v_3 + g)^2 = \frac{1}{m}U_1^2 \Rightarrow U_1 = m \cdot \sqrt{v_1^2 + v_2^2 + (v_3 + g)^2} \tag{14}$$

Using the above definition of auxiliary control inputs, as well as the definition for aerodynamics coefficients $A_x = -K_x x$, $A_y = -K_y y$, $A_z = -K_z z$, the dynamics of the translational motion of the quadropter, previously given in Eq. (7) are now written as

$$\begin{array}{c} \ddot{x} = -\frac{K_x x}{m} + v_1 \\ \ddot{y} = -\frac{K_y y}{m} + v_2 \\ \ddot{z} = -\frac{K_z z}{m} + v_3 \end{array} \tag{15}$$

or equivalently

$$\begin{pmatrix} \ddot{x} \\ \ddot{y} \\ \ddot{z} \end{pmatrix} = \begin{pmatrix} -\frac{K_x}{m} & 0 & 0 \\ 0 & -\frac{K_y}{m} & 0 \\ 0 & 0 & -\frac{K_z}{m} \end{pmatrix} \begin{pmatrix} x \\ y \\ z \end{pmatrix} + \begin{pmatrix} 1 & 0 & 0 \\ 0 & 1 & 0 \\ 0 & 0 & 1 \end{pmatrix} \begin{pmatrix} v_1 \\ v_2 \\ v_3 \end{pmatrix} \tag{16}$$

By denoting vectors $x_E = [x, y, z]^T$, $v_E = [\dot{x}, \dot{y}, \dot{z}]^T$, $F_E = [v_1, v_2, v_3]^T$, as well as by denoting matrices $K_E = diag[-\frac{K_x}{m}, -\frac{K_y}{m}, -\frac{K_z}{m}]$, $G_E = I_{3\times 3}$ one has the following concise description for the translational motion of the quadrotor

$$\begin{array}{c} \dot{x}_E = V_E \\ \dot{V}_E = K_E x_E + G_E F_E \end{array} \tag{17}$$

Moreover, in the equation about the rotational motion of the quadrotor which appears in Eq. (12) one can use the vectors definition $\dot{\eta} = \omega_E = [\phi, \theta, \psi]^T$, $\dot{\eta} = [\dot{\phi}, \dot{\theta}, \dot{\psi}]^T$, and can finally rewrite the rotational dynamics of the UAV in the form

$$\begin{array}{c} \dot{\eta} = \omega_E \\ \dot{\omega}_E = -C(\eta, \dot{\eta})\dot{\eta} + M(\eta)^{-1}\tau_\eta \end{array} \tag{18}$$

Next, by merging Eq. (17) and Eq. (18) one obtains the complete dynamic model of the quadrotor in the form

$$\begin{array}{c} \dot{x}_E = V_E \\ \dot{\eta} = \omega_E \\ \dot{V}_E = K_E x_E + G_E F_E \\ \dot{\omega}_E = -C(\eta, \dot{\eta})\dot{\eta} + M(\eta)^{-1}\tau_\eta \end{array} \tag{19}$$

Next, the state-vector of the quadrotor is defined as

$$\begin{array}{c} x = [x_E, \eta, V_E, \omega_E]^T \Rightarrow \\ x = [x, y, z, \phi, \theta, \psi, \dot{x}, \dot{y}, \dot{z}, \dot{\phi}, \dot{\theta}, \dot{\psi}]^T \Rightarrow \\ x = [x_1, x_2, x_3, x_4, x_5, x_6, x_7, x_8, x_9, x_{10}, x_{11}, x_{12}]^T \end{array} \tag{20}$$

and the control inputs vector of this UAV is defined as

$$\begin{array}{c} u = [F_E, \tau_\eta]^T \Rightarrow u = [v_1, v_2, v_3, \tau_\phi, \tau_\theta, \tau_\psi]^T \\ \Rightarrow u = [u_1, u_2, u_3, u_4, u_5, u_6]^T \end{array} \tag{21}$$

Additionally, the dynamic model the quadrotor can be written in the form of two chained subsystems after defining the state subvectors $x_{1,6} = [x_1, x_2, x_3, x_4, x_5, x_6]^T$ and $x_{7,12} = [x_7, x_8, x_9, x_{10}, x_{11}, x_{12}]^T$ as well as the following subvectors and submatrices.

$$f_{1,6}(x_{1,6}) = 0_{6\times 1} \quad g_{1,6}(x_{1,6}) = I_{6\times 6} \tag{22}$$

$$f_{7,12}(x_{1,6}, x_{7,12}) = \begin{pmatrix} K_E x_E \\ -M^{-1}(u)C((\eta, \omega_E)\omega_E \end{pmatrix} \quad g_{7,12}(x_{1,6}, x_{7,12}) = \begin{pmatrix} G_E & 0 \\ 0 & M^{-1}(\eta) \end{pmatrix} \tag{23}$$

Using the above, the dynamics of the quadrotor can be written in the form of two chained subsystems

$$\dot{x}_{1,6} = f_{1,6}(x_{1,6}) + g_{1,6}(x_{1,6}x_{7,12})x_{7,12} \tag{24}$$

$$\dot{x}_{7,12} = f_{7,12}(x_{1,6}, x_{7,12}) + g_{7,12}(x_{1,6}, x_{7,12})u \tag{25}$$

The dynamic model of the quadrotor is differentially flat with flat output vector $Y = [x_1, x_2, x_3, x_4, x_5, x_6]^T = x_{1,3}$. Indeed from Eq. (24)

$$\begin{array}{c} x_{7,12} = g_{1,6}(x_{1,6})^{-1}[\dot{x}_{1,6} - f_{1,6}(x_{1,6})] \\ \Rightarrow x_{7,12} = h_{x_{7,12}}(Y, \dot{Y}) \end{array} \tag{26}$$

This signifies that $x_{7,12}$ is a differential function of the flat outputs of the system Y. Moreover, from Eq. (25) one solves for the control inputs vector u. This gives

$$\begin{array}{c} u = g_{7,12}^{-1}(x_{1,6}, x_{7,12})[\dot{x}_{7,12} - f_{7,12}(x_{1,6}, x_{7,12})] \\ \Rightarrow v = h_v(Y, \dot{Y}) \end{array} \tag{27}$$

which signifies that u is a differential function of the flat outputs vector. Consequently, the dynamic model of the quadrotor is differentially flat.

3 Flatness-based control in successive loops for 6-DOF quadropters

It will be proven that each one of the subsystems of Eq. (24) and Eq. (25) is differentially flat and that stabilizing feedback control about them can be achieved by applying a dynamics inversion technique which is commonly used in input-output linearized systems.

For the subsystem of Eq. (24) the flat outputs vector is taken to be $Y_1 = x_{1,6}$ while $x_{7,12}$ is taken to be a virtual control input, that is $\bar{v}_1 = x_{7,12}$. Thus, solving Eq. (24) for $\bar{v}_1$ one obtains Eq. (26) which signifies that $\bar{v}_1$ is a differential function of the flat outputs Y_1. Consequently, Eq. (24) is a differentially flat subsystem.

For the subsystem of Eq. (25) the flat outputs vector is taken to be $Y_2 = x_{7,12}$ while $x_{1,6}$ is taken to be a coefficients vector and u is the real control input. Thus, solving Eq. (25) for u one obtains Eq. (27) which signifies that u is a differential function of the flat outputs Y_2. Consequently, Eq. (25) is a differentially flat subsystem.

In confirmation of the differential flatness properties of the subsystems of Eq. (24) and Eq. (25) one can notice that these subsystems are in the input-output linearized form. Consequently, control and stabilization about them can be achieved by applying common dynamics inversion techniques which have been used for input-output linearized systems.

The setpoint for the subsystem of Eq. (24) is $x_{1,6}^*$ and the stabilizing feedback control is taken to be

$$\bar{v}_1 = x_{7,12}^* = g_{1,6}(x_{1,6})^{-1}[x_{1,6}^* - f(x_{1,6}) - K_1(x_{1,6} - x_{1,6}^*)] \tag{28}$$

where K_1 is a diagonal matrix $K_1 \in R^{6\times 6}$ with diagonal elements $K_{1,ii} > 0$, $i = 1, 2, \cdots, 6$. For the subsystem of Eq. (25) the stabilizing feedback control is taken to be

$$u = g_{7,12}(x_{1,6}, x_{7,12})^{-1}[x_{7,12}^* - f_{7,12}(x_{1,6}, x_{7,12}) - K_2(x_{7,12} - x_{7,12}^*)] \tag{29}$$

where K_2 is a diagonal matrix $K_2 \in R^{6\times 6}$ with diagonal elements $K_{2,ii} > 0$, $i = 1, 2, \cdots, 6$.

By applying the control law of Eq. (28) into the subsystem of Eq. (24) and by defining the tracking error variable $e_{1,6} = x_{1,6} - x^*_{1,6}$ one obtains

$$\begin{gathered}\dot{x}_{1,6} = f_{1,6}(x_{1,3}) + g_{1,6}(x_{1,6})g_{1,6}(x_{1,6})^{-1}[x^*_{1,6} - f(x_{1,6}) - K_1(x_{1,6} - x^*_{1,6})] \Rightarrow \\ (\dot{x}_{1,6} - \dot{x}^*_{1,6}) + K_1(x_{1,6} - x^*_{1,6}) = 0 \Rightarrow \dot{e}_{1,6} + K_1 e_{1,6} = 0 \Rightarrow \\ lim_{t\to\infty} e_{1,6}(t) = 0 \Rightarrow lim_{t\to\infty} x_{1,6}(t) = x^*_{1,6}\end{gathered} \tag{30}$$

By applying the control law of Eq. (29) into the subsystem of Eq. (25) and by defining the tracking error variable $e_{7,12} = x_{7,12} - x^*_{7,12}$ one obtains

$$\begin{gathered}\dot{x}_{7,12} = f_{7,12}(x_{1,6}, x_{7,12}) + g_{7,12}(x_{1,6}, x_{7,12})g_{7,12}(x_{1,6}, x_{7,12})^{-1}[x^*_{7,12} - f(x_{7,12}) - K_2(x_{7,12} - x^*_{7,12})] \Rightarrow \\ (\dot{x}_{7,12} - \dot{x}^*_{7,12}) + K_2(x_{7,12} - x^*_{7,12}) = 0 \Rightarrow \dot{e}_{7,12} + K_2 e_{7,12} = 0 \Rightarrow \\ lim_{t\to\infty} e_{7,12}(t) = 0 \Rightarrow lim_{t\to\infty} x_{7,12}(t) = x^*_{7,12}\end{gathered} \tag{31}$$

The global stability properties of the control method can be also proven through Lyapunov analysis. To this end, the following Lyapunov function is defined

$$V = \tfrac{1}{2}[e^T_{1,6} e_{1,6} + e^T_{7,12} e_{7,12}] \tag{32}$$

It holds that $V > 0 \ \forall \ e_{1,6} \neq 0, \ e_{7,12} \neq 0$ and $V = 0$ iff $e_{1,6} = 0$, $e_{7,12} = 0$. By differentiating in time the Lyapunov function of Eq. (32) one obtains

$$\dot{V} = \tfrac{1}{2}[2e^T_{1,6}\dot{e}_{1,6} + 2e^T_{7,12}\dot{e}_{7,12}] \tag{33}$$

Moreover, by using the tracking error dynamics of Eq. (30) and Eq. (31) one obtains

$$\begin{gathered}\dot{V} = [e^T_{1,6}(-K_2 e_{1,6}) + e^T_{7,12}(-K_2 e_{7,12})] \Rightarrow \\ \dot{V} = -e^T_{1,6} K_1 e_{1,6} - e^T_{7,12} K_2 e_{7,12} \Rightarrow \\ \dot{V} < 0 \ \forall \ e_{1,6} \neq 0, \ e_{7,12} \neq 0\end{gathered} \tag{34}$$

Therefore, V is a strictly diminishing function which converges asymptotically to 0. Consequently, it holds that $lim_{t\to\infty} e_{1,6} = 0$ and $lim_{t\to\infty} e_{7,12} = 0$.

An explicit demonstration of the exponential stabilization that is achieved by flatness-based control in successive loops is given next. The Lyapunov function of the control loop is written as:

$$V = \tfrac{1}{2}[\textstyle\sum_{i=1}^{6} e_i^2 + \sum_{j=7}^{12} e_j^2] \tag{35}$$

where $e_i \ i = 1, \cdots, 6$ are the tracking errors for the state variables of the quadrotor associated with translational motion and $e_j \ j = 7, \cdots, 12$ are the tracking errors for the state variables of the quadrotor associated with rotational motion. Equivalently, the first-order time-derivative of the Lyapunov function is written as

$$\dot{V} = -[\textstyle\sum_{i=1}^{6} k_{1,i} e_i^2 + \sum_{j=7}^{12} k_{2,j} e_j^2] \tag{36}$$

where $k_{1,i} > 0 \ i = 1, \cdots, 6$ are the diagonal elements of gain matrix K_1 and $k_{2,j} > 0 \ j = 7, \cdots, 12$ are the diagonal elements of gain matrix K_2. By denoting the minimum of the above-noted elements of the feedback gain matrices as k_{min}, that is

$$k_{min} = min\{k_{1,i} : \ i = 1, \cdots, 6 \text{ and } k_{2,j} : \ j = 7, \cdots, 12\} \tag{37}$$

and using Eq. (36) one obtains that

$$\begin{gathered}\dot{V} \leq -k_{min}[\textstyle\sum_{i=1}^{6} e_i^2 + \sum_{j=7}^{12} e_j^2] \\ \Rightarrow \dot{V} \leq -2k_{min} V \Rightarrow \dot{V} + 2k_{min} V \leq 0\end{gathered} \tag{38}$$

From Eq. (38) one can demonstrate the exponential convergence of the Lyapunov function V to 0.

Remark 1: The feedback control scheme, which is followed for the cascading subsystems that constitute the dynamic model of 6-DOF quadrotor and which is based on inversion of the subsystems' dynamics of this aerial drone, is equally robust to sliding-mode control in which the switching control term has been substituted by a saturation function. One can easily confirm this for the first-order i-th subsystem of the form $\dot{x}_i = f_i(x_i) + g_i(x_i)v_i$ by defining the sliding surface $s_i = e_i = x_1 - x_i^d$ and the associated sliding mode controller $v_i = \hat{g}_i(x)^{-1}[\dot{x}_i^d - \hat{f}_i(x_i) - K_i sgn(x_i - x_i^d)]$ which after substituting the $sgn(s_i)$ function with the saturation $sat(s_i)$ function becomes $v_i = \hat{g}_i(x)^{-1}[\dot{x}_i^d - \hat{f}_i(x_i) - K_i(x_i - x_i^d)]$. The latter relation coincides with the flatness-based control in successive loops for the i-th subsystem under uncertainty (with use of the estimated functions $\hat{f}_i(x)$ and $\hat{g}_i(x)$) which is computed by the article's control method. Therefore, the proposed flatness-based control method in successive loops provides sufficient robustness margins which enable the reliable and safe functioning of the 6-DOF quadrotor under reasonable levels of model uncertainty or external perturbations.

4 Simulation tests

The flatness-based control method has been tested in different trajectory tracking scenarios for the autonomous aerial vehicle, as shown in Fig. 2 to Fig. 9, so as to confirm further the global stability properties of the control scheme that were previously proven through the article's stability analysis and to demonstrate the reliability of the new control method under variable operating conditions of the drone. As it can be seen in the associated 3D plots of the drone's helicoidal flight path under the proposed flatness-based control method in successive loops, the quadrotor follows precisely the reference trajectory and is capable of accomplishing complicated maneuvers in the 3D space. The reference trajectories in the presented 3D diagrams have been generated by considering motion of the drone on circular or ellipsoidal paths in the horizontal XY plane with simultaneous uplift motion along the Z axis under constant speed. Each flight scenario has been obtained by assuming different dimensions of the circular or ellipsoidal paths in the horizontal XY plane and different uplift velocity along the Z axis.

Indicative values about the parameters of the 6-DOF quadrotor UAV which have been used in the simulation experiments are given below: $m = 40kgr$, $g = 10m/sec^2$, $K_x = 1.1$, $K_y = 1.1$, $K_z = 1.1$, $I_{xx} = 10.6kgr{\cdot}m^2$, $I_{yy} = 10.6kgr{\cdot}m^2$, $I_{zz} = 10.6kgr{\cdot}m^2$, $I_{xy} = 0.6kgr{\cdot}m^2$, $I_{xz} = 0.6kgr{\cdot}m^2$, $I_{yz} = 0.6kgr{\cdot}m^2$. Results about the tracking accuracy and the speed of convergence to setpoints of the successive-loops flatness-based control method, in the case of the 6-DOF autonomous quadrotor, are shown in detail in Fig. 2 to Fig. 9. It can be noticed again, that under this control scheme one achieves fast and precise tracking of reference setpoints for all state variables of the dynamic model of the 6-DOF autonomous quadrotor. It is noteworthy, that through the stages of this method one solves also the setpoints definition problem for all state variables of the quadrotor. Actually, the selection of setpoints for state variables x_1 to x_6, that is $x_{1,6}^* = [x^*, y^*, z^*, \phi^*, \theta^*, \psi^*]^T$ is unconstrained. On the other side by defining state variables x_7 to x_{12} as virtual control inputs for the subsystem of state variables x_1 to x_6 one can find the setpoints for x_7 to x_{12}, denoted as $x_{7,12}^*$ as functions of the setpoints for x_1 to x_6. The speed of convergence of the state variables of the 6-DOF autonomous quadrotor when using flatness-based control implemented in successive loops is determined by the selection of values for the diagonal gain matrices $K_1 \in R^{6\times6}$, $K_2 \in R^{6\times6}$.

To elaborate on flatness-based control in successive loops for the 6-DOF UAV the following Tables are given (i) Table II providing results about the accuracy of tracking of setpoints by the state variables of the 6-DOF UAV under an exact dynamic model, (ii) Table III providing results about the accuracy of tracking of setpoints by the state variables of the 6-DOF UAV under a model that is subject to disturbances (for instance change $\Delta\alpha\%$ in the parameter which is the drag-force coefficient K_y, of the UAV's dynamic model).

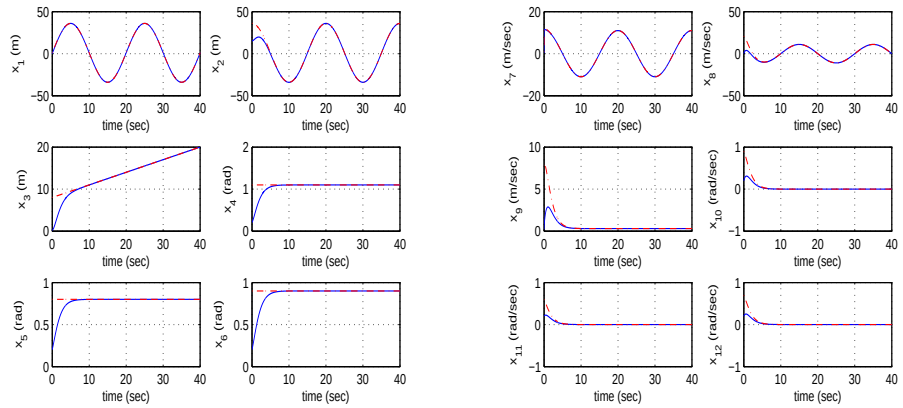

(a) **(b)**

Figure 2: Tracking of trajectory 1 by the 6-DOF autonomous quadrotor (a) convergence of state variables x_1 to x_6 to their reference setpoints (red line: setpoint, blue line: real value), (b) convergence of state variables x_7 to x_{12} to their reference setpoints (red line: setpoint, blue line: real value)

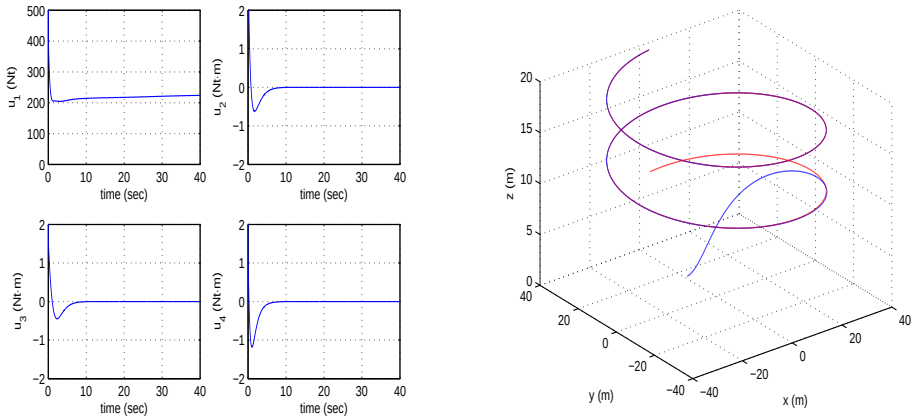

(a) **(b)**

Figure 3: Tracking of trajectory 1 by the 6-DOF autonomous quadrotor (a) variations of the thrust control input u_1 and of torque control inputs u_2 to u_4 (blue line), (b) tracking of reference trajectory (red line) by the quadrotor's position (blue line) in the XYZ cartesian space

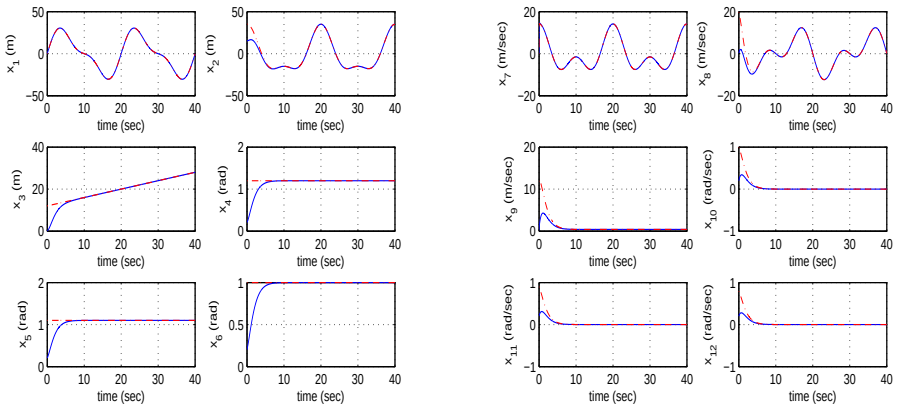

(a) **(b)**

Figure 4: Tracking of trajectory 2 by the 6-DOF autonomous quadrotor (a) convergence of state variables x_1 to x_6 to their reference setpoints (red line: setpoint, blue line: real value), (b) convergence of state variables x_7 to x_{12} to their reference setpoints (red line: setpoint, blue line: real value)

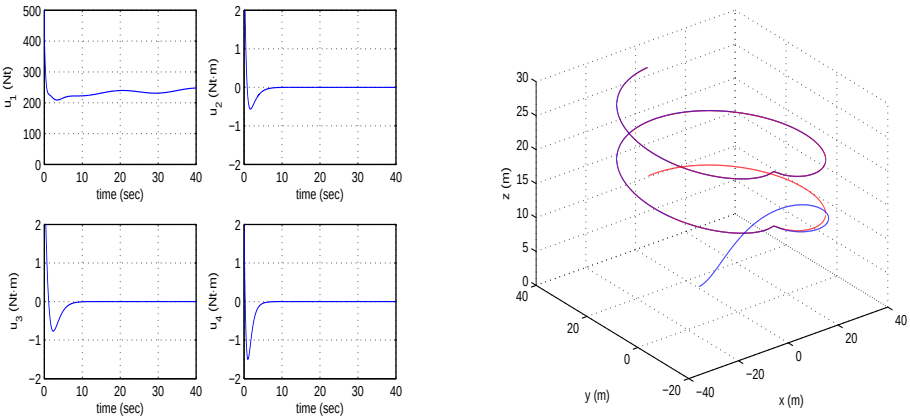

(a) **(b)**

Figure 5: Tracking of trajectory 2 by the 6-DOF autonomous quadrotor (a) variations of the thrust control input u_1 and of torque control inputs u_2 to u_4 (blue line), (b) tracking of reference trajectory (red line) by the quadrotor's position (blue line) in the XYZ cartesian space

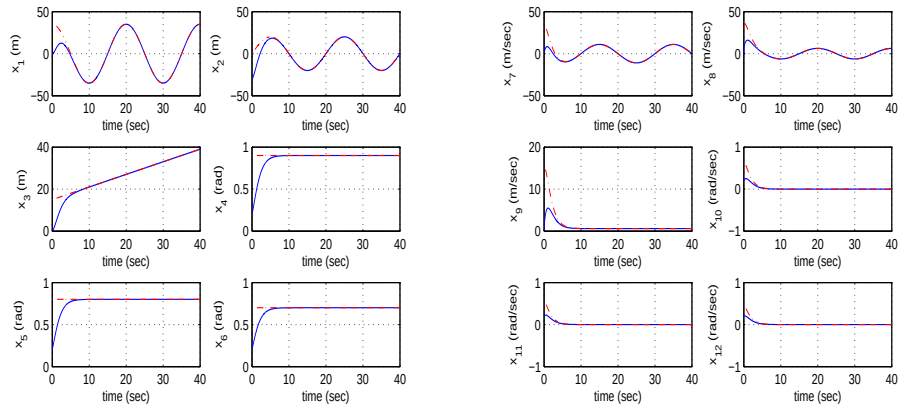

(a) **(b)**

Figure 6: Tracking of trajectory 3 by the 6-DOF autonomous quadrotor (a) convergence of state variables x_1 to x_6 to their reference setpoints (red line: setpoint, blue line: real value), (b) convergence of state variables x_7 to x_{12} to their reference setpoints (red line: setpoint, blue line: real value)

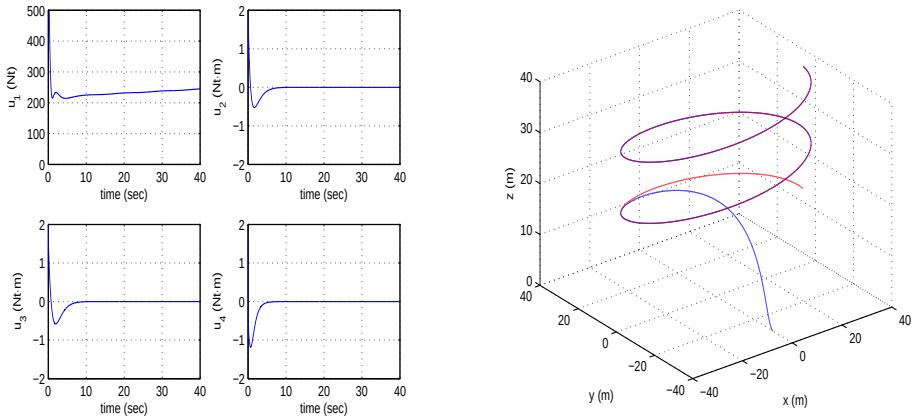

(a) **(b)**

Figure 7: Tracking of trajectory 3 by the 6-DOF autonomous quadrotor (a) variations of the thrust control input u_1 and of torque control inputs u_2 to u_4 (blue line), (b) tracking of reference trajectory (red line) by the quadrotor's position (blue line) in the XYZ cartesian space

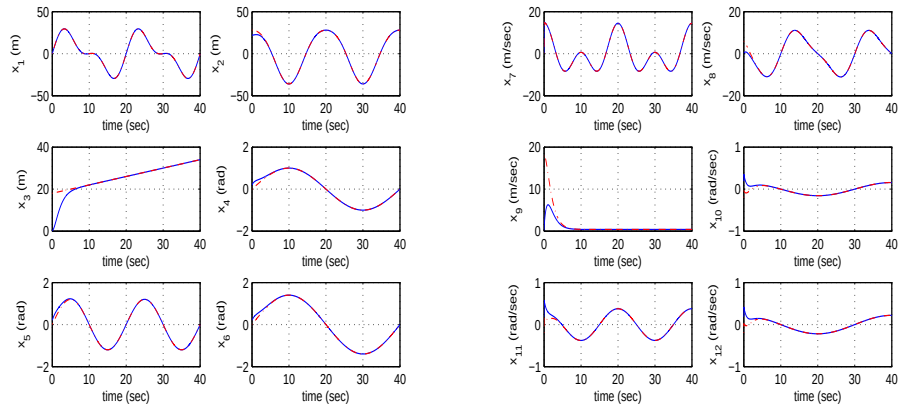

(a) **(b)**

Figure 8: Tracking of trajectory 4 by the 6-DOF autonomous quadrotor (a) convergence of state variables x_1 to x_6 to their reference setpoints (red line: setpoint, blue line: real value), (b) convergence of state variables x_7 to x_{12} to their reference setpoints (red line: setpoint, blue line: real value)

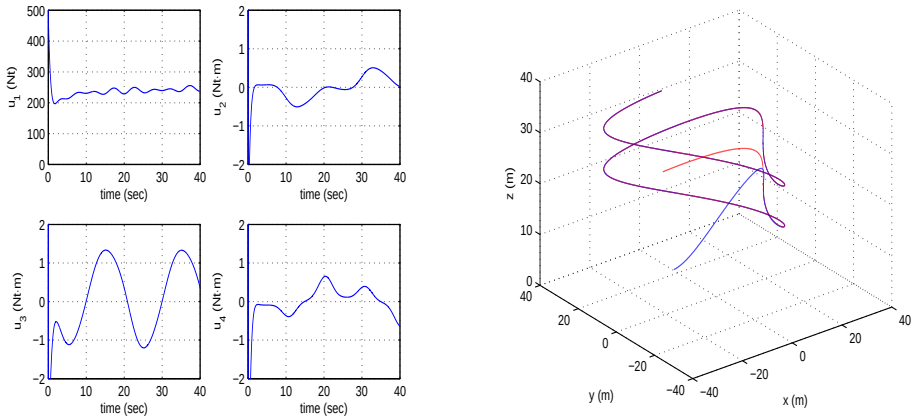

(a) **(b)**

Figure 9: Tracking of trajectory 4 by the 6-DOF autonomous quadrotor (a) variations of the thrust control input u_1 and of torque control inputs u_2 to u_4 (blue line), (b) tracking of reference trajectory (red line) by the quadrotor's position (blue line) in the XYZ cartesian space

Table II								
Tracking RMSE $\times 10^{-3}$ for the 6-DOF quadrotor UAV in the disturbance-free case								
	$RMSE_{x_1}$	$RMSE_{x_2}$	$RMSE_{x_3}$	$RMSE_{x_4}$	$RMSE_{x_5}$	$RMSE_{x_6}$	$RMSE_{x_7}$	$RMSE_{x_8}$
test_1	0.1303	0.1747	0.0001	0.0001	0.0001	0.0001	0.1058	0.0851
test_2	0.2860	0.2639	0.0001	0.0001	0.0001	0.0001	0.2453	0.3163
test_3	0.0931	0.4013	0.0001	0.0001	0.0001	0.0001	0.0756	0.5547
test_4	0.1747	0.0745	0.0001	0.0001	0.0001	0.0001	0.0951	0.0604
test_5	0.3471	0.3010	0.0001	0.0001	0.0001	0.0001	0.3248	0.4160
test_6	0.1889	0.1248	0.0001	0.0001	0.0001	0.0001	0.1512	0.0680
test_7	0.3140	0.1276	0.0001	0.0005	0.0045	0.0007	0.2782	0.0353
test_8	0.2258	0.0749	0.0001	0.0026	0.0004	0.0001	0.1745	0.0408

Table III								
Tracking RMSE $\times 10^{-3}$ for the 6-DOF quadrotor UAV in the case of disturbances								
$\Delta a\%$	$RMSE_{x_1}$	$RMSE_{x_2}$	$RMSE_{x_3}$	$RMSE_{x_4}$	$RMSE_{x_5}$	$RMSE_{x_6}$	$RMSE_{x_7}$	$RMSE_{x_8}$
0%	0.1889	0.1248	0.0001	0.0001	0.0001	0.0001	0.1512	0.1680
10%	0.2000	0.1000	0.1000	0.1000	0.1000	0.1000	0.2000	1.3000
20%	0.2000	0.2000	0.1000	0.1000	0.1000	0.1000	0.2000	2.6000
30%	0.2000	0.4000	0.1000	0.1000	0.1000	0.1000	0.2000	4.0000
40%	0.2000	0.5000	0.1000	0.1000	0.1000	0.1000	0.2000	5.3000
50%	0.2000	0.7000	0.1000	0.1000	0.1000	0.1000	0.2000	6.6000
60%	0.2000	0.9000	0.1000	0.1000	0.1000	0.1000	0.2000	8.0000

The concept of flatness-based control in successive loops is clearly analyzed in the article. The state-space model of the controlled system, being in the triangular (backstepping integral) form, is decomposed into a chain of subsystems which are connected in a cascading form, that is the state vector of the $(i+1)$-th subsystem becomes virtual control inputs vector for the i-th subsystem. Equivalently, the value of the virtual control inputs vector which stabilizes the i-th subsystem becomes setpoint for the state vector of the $(i+1)$-th subsystem. For each subsystem differential flatness properties are proven, signifying that it can be written in the input-output linearized form and the stabilizing feedback control about it can be designed by inverting its dynamics. The global stability properties of this control scheme are proven analytically through the equations that give the tracking error dynamics of this system. They are also proven through Lyapunov stability analysis.

The presented flatness-based control method in successive loops for 6-DOF quadrotor UAVs is based on an exact linearization procedure of the dynamics of the controlled system without being subjected to the flaws of global linearization procedures, that is the need to perform changes of state variables and complicated transformations of state-space descriptions. Therefore, comparing to global linearization-based control approaches, for instance (i) Lie algebra-based control which requires the extended computations of the so called Lie-derivatives of the state-space model of the system and (ii) typical implementations of flatness-based control which require successive differentiations of the flat outputs of the system so as to arrive at an input-output linearized form or at canonical Brunovsky's forms, the article's flatness-based control method in successive loops is applied directly on the initial nonlinear state-space model of the system and does not require any state-space model transformations. Additionally, in comparison to control methods which use approximate linearization of the state-space model of the controlled system, as for instance methods of multi-model fuzzy control methods that linearize locally the controlled system around operating points and compute controllers associated with the local linear models, the article's approach does not introduce any modelling errors and does not have to compensate for model uncertainty induced by the linearization process. It is also noted that the article's flatness-based control method in successive loops is of proven global

stability and of associated robustness margins, which is not the case for other popular control schemes for industrial systems such as PID control and Nonlinear Model Predictive Control. Actually, PID control is mostly relying on an empirical selection of the feedback gains of the controller so as to achieve satisfactory performance around a specific operating point. Changes of the operating conditions or exogenous perturbations can destabilize PID control loops. Furthermore, in NMPC methods the convergence of the iterative search for an optimum is dependent also on empirical selection of controller parameters and on initialization (multiple shooting methods) while also lacking a global stability proof.

Remark 2: The proposed flatness-based control method in successive loops has good potential for use at the industrial scale and in a wide class of robotic systems. This control method can be used in all robotic systems which can be written in the triangular (strict-feedback) state-space form after decomposing their initial state-space description into a series of chained subsystems. Among various application domains one can note several types of robotic manipulators, such as multi-DOF robotic arms with rigid links and electric, electro-hydraulic or electro-pneumatic actuators, robotic manipulators with flexible joints, special types of robots such as SCARA robots, parallel robots, redundant robotic manipulators and gantry cranes. Besides, one can note several types of autonomous vehicles in which the flatness-based control method in successive loops is applicable. These include, autonomous ground vehicles such as four-wheel car-like vehicles and three-wheel omnidirectional robots, unmanned aerial vehicles such as quadrotors, tilt-rotor UAVs and octocopters, aerospace systems such as autonomous reentry vehicles and satellites, autonomous underwater vessels such as 3-DOF submersible autonomous robots and 6-DOF submarines. The flatness-based control method in successive loops is characterized by the avoidance of complicated state-space model transformation and simplicity in the computation of the stabilizing feedback control gains which take the form of some positive diagonal matrices.

Remark 3: One can certainly consider a state estimation-based approach for controlling the 6-DOF autonomous quadrotor in which the flatness-based controller in successive loops stabilizes the UAV and makes it track precisely the designated flight paths after using feedback of the estimated state vector of the drone which is obtained with the use of a nonlinear filtering technique.The nonlinear H-infinity Kalman Filter is a robust-to-noise state estimator which can be used for this purpose. This filter is based on linearization of the drone's dynamic model through the computation of the associated Jacobian matrices. This linearization takes place at each sampling instant around a time-varying setpoint which is defined by the present value of the system's state vector and by the last sampled value of the control inputs vector.

Remark 4: The so-called backstepping control, which is based on the recursive computation of the control signal of the system after applying virtual control inputs to the individual rows of the state-space model, can be completely substituted by the proposed flatness-based control method. A backstepping control law can be derived for systems of the triangular form. However, as it was previously analyzed, by showing that each row of the state-space model stands for a subsystem that satisfies differential flatness properties one can apply effectively to each subsystem the controller design stages found in input-output linearizing flatness-based control methods.

5 Conclusions

The article has analyzed a novel solution to the problem of nonlinear control of 6-DOF autonomous quadrotors, without the need to apply changes of state variables (diffeomorphisms) and complicated state-space transformations. The new solution is a flatness-based control approach implemented in successive loops. The proposed control method in successive loops can be used in all autonomous aerial vehicles which have a state-space model in the strict feedback (backstepping integral) form or to systems which can be transformed to such a form. The method can be applied through the same implementation stages to more types of aerial drones, such as several types of rotorcrafts, fixed-wing aircrafts and helicopters. So

far the flatness-based control method in successive loops has been tested in autonomous quadrotors and octocopters, fixed-wing VTOLs, and tilt-rotor UAVs.

In flatness-based control in successive loops the dynamic model of the nonlinear system is separated into cascading subsystems which satisfy differential flatness properties. For each subsystem of the state-space model a virtual control input is defined, capable of inverting the subsystem's dynamics and of eliminating the subsystem's tracking error. The control input which is actually applied to the initial nonlinear system is obtained from the last row of the state-space description. This control input incorporates in a recursive manner all virtual control inputs which were computed from the individual subsystems included in the initial state-space equation. The global stability properties of the new control method have been analytically proven with the use Lyapunov stability analysis, while exponential convergence has been also confirmed.

Statement: This research work has been partially supported by Grant Ref. 301022 "*Nonlinear optimal and flatness-based control methods for complex dynamical systems*" of the Unit of Industrial Automation of the Industrial Systems Institute.

References

[1] Rigatos G., 2016, "Nonlinear control and filtering using differential flatnesss theory approaches: Applications to electromechanical systems", Springer.

[2] Rigatos G. and Busawon K., 2018, "Robotic manipulators and vehicles: Control, estimation and filtering", Springer.

[3] Rigatos G., Abbaszadeh M., Siano P., 2022, "Control and estimation of dynamical nonlinear and partial differential equation systems: Theory and Applications", IET Publications.

[4] Rigatos G. and Karapanou E., 2020, "Advances in applied nonlinear optimal control", Cambridge Scholars Publishers.

[5] Levine, J., 2009, "Analysis and Control of Nonlinear Systems: A flatness-based approach", Springer.

[6] Riachy S., Fliess M., Join C. and Barbot J.P. 2010, "Vers une simplification de la commande non linéaire : l'exemple d'un avion à décollage vertical". Sixième Conférence Internationale Francophone d'Automatique, CIFA 2010, Jun 2010, Nancy, France.

[7] Fliess M. and Mounier H., 1999, "Tracking control and π-freeness of infinite dimensional linear systems", In: G. Picci and D.S. Gilliam Eds.,Dynamical Systems, Control, Coding and Computer Vision, 258, pp. 41-68, Birkhaüser.

[8] Villagra J., d'Andrea-Novel B., Mounier H. and Pengov M., 2007, "Flatness-based vehicle steering control strategy with SDRE feedback gains tuned via a sensitivity approach", IEEE Transactions on Control Systems Technology, 15, pp. 554-565.

[9] Bououden S., Boutat D., Zheng G., Barbot J.P. and Kratz F., 2011, "A triangular canonical form for a class of 0-flat nonlinear systems", International Journal of Control, Taylor and Francis, 84(2), pp. 261-269.

[10] Menhour L., d'Andre'a-Novel B., Fliess M. and Mounier H., 2014, "Coupled nonlinear vehicle control: Flatness-based setting with algebraic estimation techniques", Control Engineering Practice, Elsevier, 22, pp. 135–146.

[11] Nicolau F., Respondek W. and Barbot J.P, 2022, "How to minimally modify a dynamical system when constructing flat inputs", Internattional Journal of Robust and Nonlinear Control, 31(18), pp. 9538-9561, J. Wiley.

[12] Letelier C. and Barbot J.P., 2021, "Optimal flatness placement of sensors and actuators for controlling chaotic systemsm Chaos", AIP Publications, 31(10), article No 103114.

[13] Sira-Ramirez H. and Agrawal S., 2004, "Differentially Flat Systems", Marcel Dekker, New York.

[14] Lévine J., 2011, "On necessary and sufficient conditions for differential flatness", Applicable Algebra in Engineering, Communications and Computing, Springer, 22(1), pp. 47-90.

[15] Nicolau F., Respondek W. and Barbot J.P., 2021, "Construction of flat inputs for mechanical systems", 7th IFAC Workshop on Lagrangian and Hamiltonian methods for nonlinear control, Berlin, Germany.

[16] Limaverde Filho J.O., Fortaleza E.C.R. and Campos M.C.M., 2021, "A derivative-free nonlinear Kalman Filtering approach using flat inputs", International Journal of Control, Taylor and Francis, 95(11): 2900-2910.

[17] Barbot J.P., Fliess M. and Floquet T., 2007, "An algebraic framework for the design of nonlinear observers with uknown inputs", IEEE CDC 2007, IEEE 46th Intl. Conference on Decision and Control, New Orleans, USA.

[18] Khalil H., 1996 , Nonlinear Systems, Prentice Hall.

[19] Rigatos G.G. and Tzafestas S.G., 2007, "Extended Kalman Filtering for Fuzzy Modelling and Multi-Sensor Fusion", Mathematical and Computer Modelling of Dynamical Systems, Taylor & Francis), 13(3), pp. 251-266.

[20] Basseville M. and Nikiforov I., 1993, "Detection of abrupt changes: Theory and Applications", Prentice-Hall.

[21] Rigatos G. and Zhang Q., 2009, "Fuzzy model validation using the local statistical approach", Fuzzy Sets and Systems, Elsevier, vol. 60, no. 7, pp. 882-904, 2009.

[22] Chamseddine A., Zhang Y., Rabbath C.A., Join C. and Theilliol D., 2012, "Flatness-based trajecotry planning / replanning for a quadrotor unmanned aerial vehicle", 48(4), pp. 2832-2848.

[23] Lee T, 2017, "Geometric control of quadrotor UAVs transporting a cable-suspended rigid body", IEEE Transactions on Control Systems Technology, 26(1), pp. 259-264, 2017

[24] Yu X., Zhou X., Guo K., Jia J., Guo L. and Zhang Y., 2022, "Safety flight control fir a quadrotor UAV using differential flatness and dual-loop observers", IEEE Transactions on Industrial Electronics, 69(12), pp. 13326-13336.

[25] Tognon M., Dash S.S. and Franchi A., 2016, "Observer-based control of position and tension for an aerial robot tethered toa moving platform", IEEE Robotics and Automation Letters, 1(2), pp. 732-737.

[26] Chamseddine A., Theilliol D., Zhang Y.M., Join C. and Rabbath C.A., (2015), "Active fault tolerant control system design with trajectory re-planning against actuator fault and saturation: Application to a quadrotor command aerial vehicle", Intl. Journal of Adaptive Control and Signal Processing, J. Wiley, 29, pp. 1-23, 2015.

[27] Ogunbodede O., Nandi S. and Signh T., 2019, "Periodic control of unmanned aerial vehicles based on differential flatness", ASME Journal of Dynamical Systems Measurement and Control, 141(7), pp. 071003: 1-10.

[28] Abadi A., El-Amraoui A,, Mekki H., and Ramdani N., 2020, "Robust tracking control of quadrotor based on flatness and active disturbance rejection control, IET Control Theory and Applications, 14(8), pp. 1057-1068.

[29] Rigatos G., Siano P. and Zervos N., 2015, "A new concept of flatness-based control of nonlinear dynamical systems", IEEE INDIN 2015, 13th IEEE Intl. Conf. on Industrial Informatics, Cambridge, UK.

[30] Rigatos G., Siano P., Ademi S. and Wira P., 2010, "Flatness-based control of DC-DC converters implemented in successive loops", Electric Power Components and Systems, Taylor and Francis, 46(6), pp. 673-687.

[31] Zhang Y.M., Chamzeddine A., Rabbath, B.W. Gordon, C.Y. Su, S. Rakheja, C. Fulford, J. Apkarian and R. Gosselin, 2013, "Development of advanced FDD and FTC techniques with application to an unmanned quadrotor helicopter testbed", Journal of the Franklin Institute, Elsevier, vol. 360, pp. 2396-2422, 2013.

[32] Martins L., Cordeira C. and Oliveira, 2012, "Feedback linearization with zero dynamics stabilization for quadrotor control, Journal of Intelligent and Robotic Systems", Springer, 101(7), pp. 1-17.

[33] Sheng Y.and Tao G., 2021, "System characterization and adaptive tracking control of quadrotors under multiple operating conditions", Journal of Guidance, Navigation and Control, World Scientific, 1(2), pp. 2150006-2150045.

[34] Ghandour J., Aberkan S. and Ponsart J.C., 2014, "Feedback linearization approach for standard and fault tolerant control: Application to a Quadrotor UAV testbed", Journal of Physics: Conference Series, vol. 570, no. 082003, pp. 1-12.

[35] Dolwadi N., Dob D. and Muyeen S.M., 2022, "Adaptive backstepping controller design of quadrotor biplane for payload delivery", IET Intelligent Transportation Systems, 16(2) pp. 1738-1752.

[36] Machida S., Matsuda R., Ibuki J. and Sampei M., 2021, "A geometric control of hoverability analysis for multirotor UAVs with upward oriented rows", IEEE Transactions on Robotics, 37(5) pp. 1765-1779.

[37] Diaz-Mendez Y., de Jesus L.D., de Sousa M.S., Counha S.S. and Ramos A.B., 2021, "Conditional integrator sliding-mode controller of an unmanned quadrotor helicopter", Proc. IMechE - Part I: Journal of Systems and Control Engineering, 236(3), pp. 458-472.

[38] Ofadile N.A. and Turner M.C., 2016, "Decentralized approaches to antiwind-up design with apppli-cation to quadrotor unmanned aerial vehicle", IEEE Transactions on Control Systems Technology, 24(6), pp. 1980-1992.

[39] Jin X., Tang Y., Shi Y., Zhang W. and Du W., 2022, "Event-triggered formation control for a class of uncertain Euler-Lagrange systemsL Theory and Experiment", IEEE Transactions on Control Systems Technology, 30(1), pp. 336-343.

[40] Yu X., Zhou X., Guo K., Jin J., Gio K. and Zhang Y., 2022, "Safety flight control for a quadrotor UAV using differential flatness and dual-loop observer", IEEE Transactions on Industrial Electronics, 69(12), pp. 13336-13335.

[41] Ai X. and Yu J., 2019, "Fixed-time trajectory tracking for a quadrotor with external disturbances: A flatness-based sliding-mode control approach", Aerospace Science and Technology, Elsevier, 89, pp. 58-76.

[42] Ma D., Xia Y., Shou G., Jia Z. and Li T., 2022, "Flatness-based adaptive sliding-mode tracking control for a quadrotor with disturbances", Journal of the Franklin Institute, Elsevier, 355(14), pp. 6300-6322.

[43] Baldini A., Felicetti R., Freddi A., Longhi S., Monteriu A. and Rigatos G., 2019, "Actuator fault tolerant position control of a quadrotor unmanned aerial vehicle", IEEE Systol 2019, 4thb IEEE Conference on Control and Fault Tolerant Systems, Casablanca, Morocco.

[44] Wang J., Boussaada I., Cela A, Mounier H. and Niculescu S.I., 2012, "Analysis and control of quadrotor via a normal form approach", IEEE Intl. Symposium on Mathematical Theory of Networks and Systems, Melbourne, Australia.

[45] Freddi A., Lanzon A. and Longhi S., "A feedback linearization approach to fault tolerance in quadrotor vehicles", 18th IFAC World Congress, Milan, Italy.

[46] Rigatos G. and Siano P., 2015, "A New Nonlinear H-infinity Feedback Control Approach to the Problem of Autonomous Robot Navigation", Journal of Intelligent Industrial Systems, Springer, 1(3), pp. 179-186.

[47] Raffo G.V., Ortega M.G. and Rubio F.R., 2010, "An integral predictive/nonlinear H_∞ control structure for a quadrotor helicopter", Automatica, Elsevier, 46(1), pp. 29-39.

[48] Lendek Z., Berna A., Guzman-Gimenez J., Sala A. and Garcıa P., 2011, "Application of Takagi-Sugeno observers for state estimation in a quadrotor", 2011 CDC-ECC, 50th IEEE Conference on Decision and Control and European Control Conference Orlando, FL, USA.

[49] Lee T., 2012, "Robust Adaptive Attitude Tracking on SO(3) With an Application to a Quadrotor UAV", IEEE Transactions on Control Systems Technology, 2(5), pp. 1924-1930.

[50] Wang Y., Guan Y., Li H., 2023, "Spiking-Free Disturbance Observer-Based Sliding-Mode Control for Mismatched Uncertain System", Journal of Dynamic Systems, Measurement and Control, doi.org/10.1115/1.4063609, pp. 1-17.

[51] He Y., Pei H., and Sun T., 2014, "Robust tracking control of helicopters using backstepping with disturbance observers", Asian Journal of Control, 16(6), pp. 1–16.